CONTROL SYSTEMS OF THE NASA 70-METER ANTENNAS

W. Gawronski, H.G. Ahlstrom, Jr., and A.M. Bernardo
Jet Propulsion Laboratory, California Institute of Technology
Pasadena, California 91109

The control systems of the NASA 70-m antennas include the antenna control system, the Master Equatorial control system, and their combinations (called modes). The Master Equatorial is a small telescope mounted on the top of a tower located inside the antenna structure. In the Antenna Encoder mode antenna encoders are used to close the feedback loop. In the Autocollimator mode the Master Equatorial is a master that follows a target, and the antenna is a slave that follows the Master Equatorial. In the Master Equatorial Encoder mode the "master-slave" relationship is reversed. In the paper the analysis begins with the description of the open loop models of the antenna and of the Master Equatorial. We obtained the models by using field test data and system identification techniques. Next, we analyzed and evaluated the performance of the three modes of the antenna control system. The analysis showed that the Autocollimator and Master Equatorial Encoder tracking modes are feasible for high-rate tracking, and that the latter mode has the smallest tracking error. Finally, we analyzed the switching between antenna modes, necessary while tracking near the keyhole. We showed that switching causes jerks of magnitudes within the acceptable threshold.

1. Introduction

The NASA Deep Space Network antennas are used to communicate with spacecraft by sending commands to a spacecraft (uplink) and by receiving information from spacecraft (downlink). The antennas are located at three sites: Goldstone (California), Madrid (Spain), and Canberra (Australia) to assure continuous tracking of spacecraft during Earth rotation. The signal frequency is 2GHz (S-band), 8 GHz (X-band), or 32 GHz (Ka-band). The dish size of the antennas is either 34 meters or 70 meters. An example of the 70-meter antenna is shown in Fig.1. The antenna dish rotates with respect to horizontal axis (called elevation axis). The whole antenna structure rotates on a circular track (azimuth track) with respect to the vertical axis (called azimuth axis). For the Ka-band, the required tracking accuracy is on the order of 1 mdeg. This requirement is a driver for the control system upgrade of the 70-meter antennas. For the antenna pointing challenges see Ref.[1].

The 70-meter antenna control system consists of the antenna controller itself and of the Master Equatorial (ME) control system. The ME is a small telescope mounted on the top of a tower located inside the antenna structure, see Fig.2. The intention was to locate the ME close to the focal point of the antenna. An optical instrument called an autocollimator creates an optional link between the antenna dish and the ME. The ME is a master: it is commanded to follow a target; and the antenna is a slave: it follows the ME using an optical coupling of the autocollimator. This configuration of the antenna and the ME control systems is called the autocollimator (AC) mode.

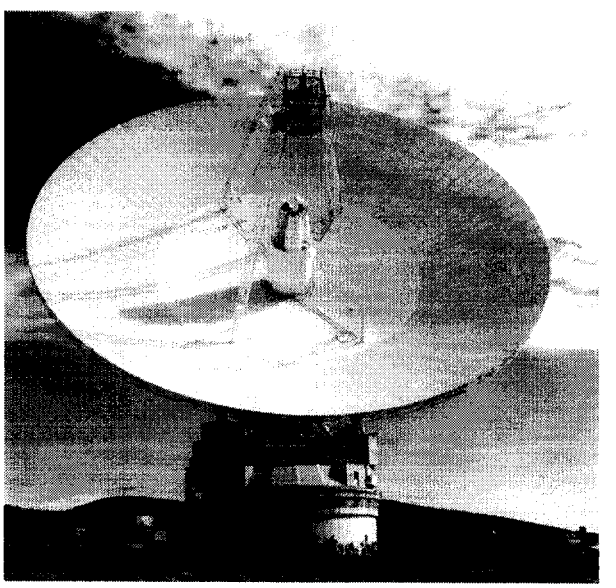

Figure 1. 70-meter antenna at Goldstone, California.

The antenna can use the azimuth and elevation encoders instead of the autocollimator. This configuration is called antenna encoder (AE) mode. The encoders – although relatively precise – cannot exactly measure the actual beam position due to their distant location from the beam focal point, while the ME and the autocollimator are located closely to the RF beam location.

In certain situations (e.g., near the antenna keyhole, or singular point) the antenna, as a slower device, may lag behind the ME and stay out of the range of the autocollimator. In this case the control system switches from the autocollimator to the encoders so that tracking

is not interrupted. The switching causes antenna jerking (since different algorithms control autocollimator and encoder modes), and loss of tracking precision. In the paper we present a new combination of the antenna and ME control systems, called the MEE (ME encoder) mode. This mode improves tracking precision, minimizes switching during tracking, and prevents extensive oscillations and jerking during switching. The MEE mode is a reconfigured antenna control system, such that the ME is a slave and follows the antenna. In effect it serves as a position sensor. In this mode the ME, a low inertia and fast device, virtually never lags significantly behind the antenna.

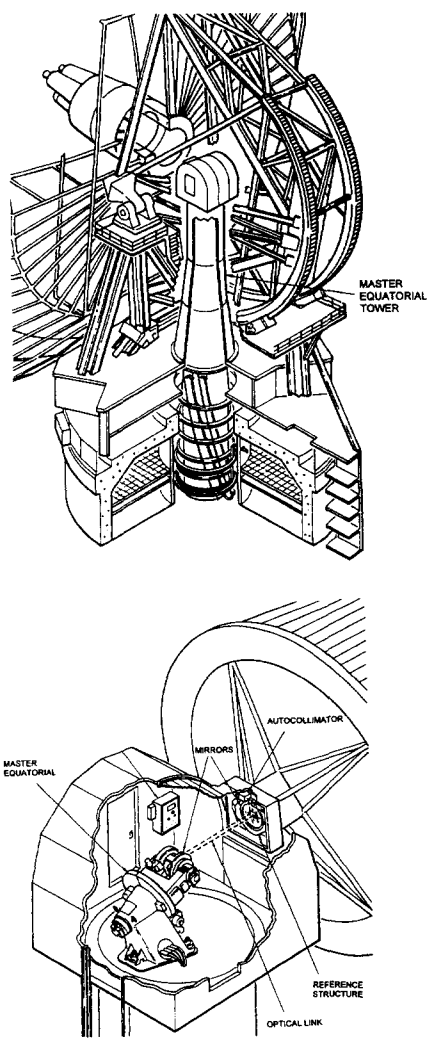

Figure 2. Master Equatorial system: (a) ME tower and (b) ME, autocollimator and mirrors.

The controller design requirements is to reduce the servo error in 32 km/h wind below the current 2.7 mdeg (rms), the servo error during controller switching shall be less than ±110 mdeg, max rate is 0.25 deg/s, and max acceleration is 0.2 deg/s^2.

The contribution of this paper includes the development of the open-loop antenna model using field data and system identification procedures, the development of the LQG control algorithm for the 70 meter antenna, the development of two control cooperating systems (antenna and ME) and proving that both are adequate for antenna tracking, but identifying the more appropriate, and analyzing of switching between two control systems.

In order to carry on the analysis, first we give details on the antenna open-loop model and ME open loop model. Next, we present the results of design of the antenna and of ME controllers, which followed by the description and performance of the two modes of the antenna and ME control systems. Finally, we analyze the switching from AC or MEE mode to AE mode.

2. Open-Loop Models

The block diagram of the current control system of a 70-meter antenna is shown in Fig.3. It consists of the following subsystems:

- autocollimator (an optical instrument that measures the position of the antenna dish),
- the antenna open-loop subsystem (antenna structure and the drives),
- antenna controllers
- a switch that alters the controllers.
- ME open loop subsystem (ME instrument and its drives),
- ME controller.

We used field tests and the system identification procedure to determine the open-loop models of the antenna and of the ME. We used these models in the antenna and ME controller design. The antenna tests supplied information on structural resonances, and on differences between the encoder loop (encoders used as sensors) and autocollimator loop (autocollimator used as sensor). The locations of the test signal injection and the locations of the test points for the antenna and ME tests are shown in Fig.3.

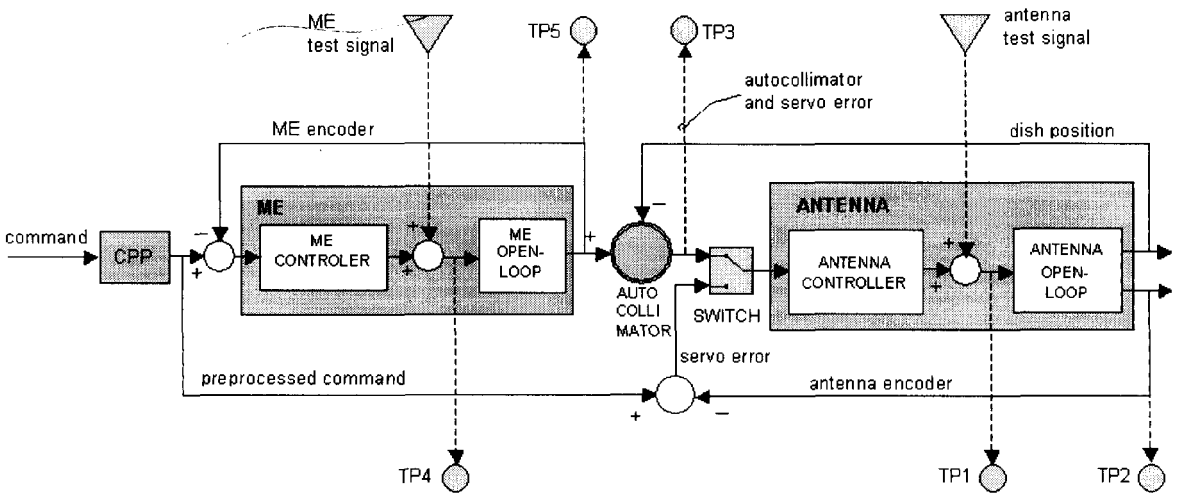

Figure 3. The existing configuration of the antenna and ME: Antenna encoder (AE) mode – when switch is at lower position, autocollimator (AC) mode when switch is at upper position; test points are denoted TP, and signal injection points marked with triangles.

2.1. Open-Loop Antenna Model

We obtained the open-loop antenna model using field tests and the system identification procedure. For the testing purposes we applied white noise; the noise is "white", if its bandwidth is much larger than the bandwidth of the test article. The open-loop antenna bandwidth does not exceed 10 Hz; therefore (according to the Nyquist criterion) the selected the noise bandwidth of 23 Hz serves the purpose. The test records are divided into sections and averaged; therefore the longer the record, the better. Our experience shows that the record of 2^{14}=16382 samples results in satisfactory accuracy of the signal processing, while shorter records produce rather noisy results.

White noise is injected into the closed-loop system, at the location denoted "antenna test signal", in Fig.3. We recorded the input voltage for the azimuth or elevation axis at test point TP1 in Fig.3, along with azimuth or elevation encoders (test point TP2 in Fig.3), and the autocollimator hour angle and declination angle readings (test point TP3 in Fig.3).

Next, we determined the open-loop transfer function using the input and output data, and the Matlab procedure *spectrum*. The input signal at point TP1 is denoted by u. The output y is the response of the encoder or the autocollimator.

The sampling time Δt (or sampling frequency $f_o = 1/\Delta t$) defines the highest frequency f_c of the transfer function. This band-limiting frequency or Nyquist frequency is half of the sampling frequency $f_c = \frac{1}{2\Delta t} = \frac{f_o}{2}$. In our case $\Delta t = 0.0435$, ($f_o = 23$ Hz), thus f_c =11.5 Hz.

The frequency resolution of the spectra, Δf, is obtained from the length of the record (N) and from the sampling time (Δt), namely $\Delta f = \frac{1}{N\Delta t} = \frac{f_o}{N}$. It is, at the same time, the lowest frequency of the spectra. In our case the total length of the record was divided into 16 segments of 1024 samples, and $f_o = 23$ Hz, thus $\Delta f = 0.0225$ Hz.

The estimate of the transfer function between the rate input and the autocollimator is plotted in Figure 4, as a dashed line. It shows a slope of 20 dB/dec and phase of –90 deg in the low frequency range. A resonance peak is visible at frequency 1.1 Hz, and noise above 5 Hz. From the collected input and output data we determined the state space representation of the open-loop model. We used the SOCIT code of the NASA Langley Research Center, see manual, Ref. [2], and the method is described in Ref.[3]. The results of the system identification are presented in Fig.4: the solid line plot represents the transfer function of the identified azimuth axis model. Magnitudes of the transfer functions for the elevation open-loop were determined in a similar way.

Figure 5 shows the system identification results for the autocollimator output and for the azimuth encoder output. Note that the resonance peaks are much higher at the autocollimator location than at the encoder locations, since the alidade (lower structure) vibrations at this frequency are more intensive at the top than at the bottom (where azimuth encoder is located). It also

points that the encoders are not good devices to sense the flexible motion of the antenna at the focal point.

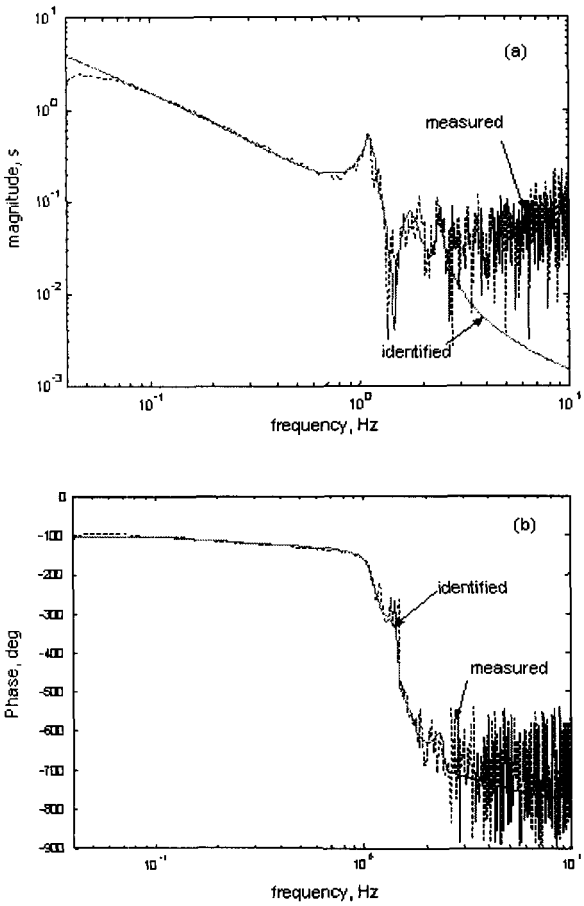

Figure 4. DSS14 azimuth axis autocollimator mode transfer function: (a) magnitude, and (b) phase.

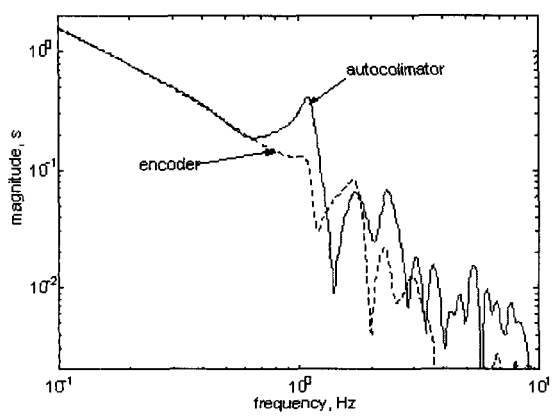

Figure 5. Magnitudes of the DSS14 azimuth axis transfer function for the autocollimator and the azimuth encoder

2.2. Open-Loop Master Equatorial Model

Similarly to the antenna model, we obtained the open-loop ME model using field tests and the system identification procedure. The ME test points are marked TP4 and TP5 in Fig.3. The input signal at point TP4 represents total input to the ME (it consists of the ME test signal and the feedback signal), and the ME encoder is recorded at point TP5. Note that ME is a rigid instrument; therefore, within 10-Hz antenna bandwidth it behaves as an integrator. Indeed, consider the transfer function of the ME hour axis of the DSS14 antenna in Fig.6. The slope of the transfer function magnitude is –20 dB/dec (the phase was -90 deg). These are values representing an integrator, or a rigid body structure.

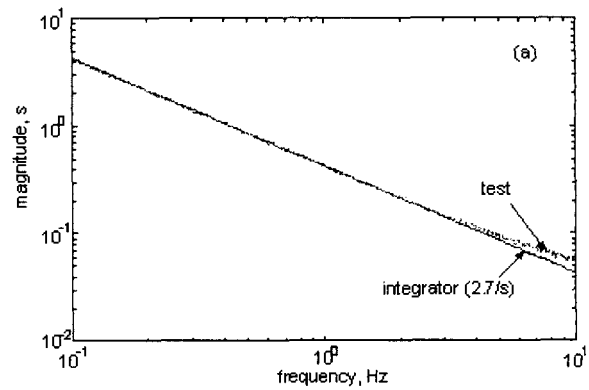

Figure 6. Magnitude of the DSS14 ME transfer functions, hour axis.

3. Closed-Loop Systems

In this section we describe the antenna and ME closed-loop systems, and characterize their performance. The closed-loop performance is characterized in terms of step responses, of transfer functions, and of wind disturbance rejection.

3.1. Antenna Closed-Loop System

Currently four control algorithms resided in the Antenna Servo Controller:

(1) a slew algorithm
(2) an encoder tracking algorithm
(3) an autocollimator tracking algorithm
(4) switching algorithm.

The slew algorithm is used for large angle slewing. In this case the rate and acceleration limits are reached and may cause instability due to antenna nonlinear behavior. In the encoder algorithm the encoder feedback is used to track spacecraft. It is used when the autocollimator is outside signal acquisition range, e.g., when antenna is commanded at rates surpassing

maximum allowable rate. In the autocollimator mode the antenna uses autocollimator feedback to follow the Master Equatorial. The last algorithm is a special algorithm used to switch from one algorithm to another, see Ref. [6].

Our objective is to introduce a single control algorithm for the encoder and autocollimator outputs and for slewing. There are three reasons that four different algorithms have to be used:

(1) the rate and acceleration limits are reached,
(2) the switching algorithm is necessary because each mode is controlled by separate control algorithms.
(3) the autocollimator error exceeds ±110 mdeg, or 220 mdeg peak-to-peak.

We implemented a command preprocessor algorithm to solve the first problem. With introduction of the command preprocessor there is no need for a separate slewing and control algorithms. A command preprocessor (CPP) is described in Ref. [7]. It prevents the antenna commands to exceed the imposed rate and acceleration limits (of 0.25 deg/s and 0.2 deg/s^2, respectively).

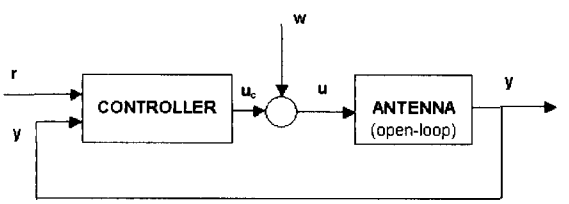

Figure 7. Closed-loop system, AE mode: r – command, y – encoder position, u_c – controller output, w – wind disturbance, and u – open loop input.

We implemented identical control algorithms for the encoder and for the autocollimator modes to solve the second problem. Switching in this case causes minimal jerk.

We solved the third problem by the implementing of the linear-quadratic-Gaussian (LQG) controller. This controller reduces the autocollimator error to less than 220 mdeg. The application of the LQG controller for the antenna tracking purposes is described in Ref.[4], and the LQG controller design process was described in Refs. [5] and [6]. The LQG control system structure is shown in Fig.7. It consists of the antenna open-loop system (antenna structure and the drives) obtained from the system identification tests, and of a controller. Antenna LQG controller is shown in Fig.8. It is split into proportional-and integral part (k_p and k_i gains), and flexible mode part (k_f gain). Separate LQG controllers were designed for azimuth and elevation axes. Their performance is evaluated in terms of step responses, transfer function bandwidth, and rms servo error due to wind gusts.

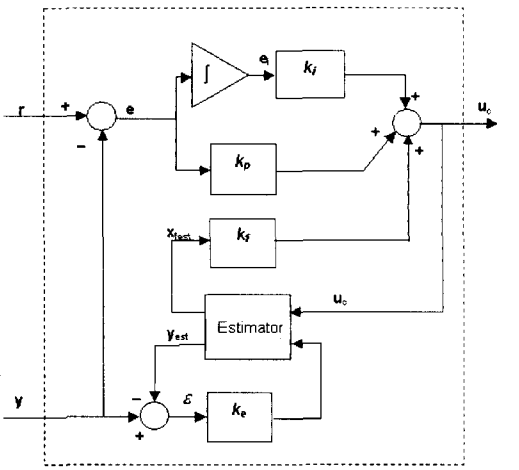

Figure 8. Antenna LQG controller: k_p – proportional gain, k_i – integral gain, k_f – flexible mode gain, k_e – estimator gain, r – command, y – encoder position, y_{est} – estimated encoder position, x_{fest} – estimated flexible mode dynamics, e – servo error, e_i – integral of the servo error, ε – estimation error, and u_c – controller output.

Azimuth axis controller performance. The responses to the 10-mdeg step of the azimuth encoder and the azimuth autocollimator are shown in Fig.9. The settling time in both cases is 2 s, overshoot is 44% at autocollimator and 32% at encoder. The magnitudes of the closed-loop transfer functions are shown in Fig.10, for the autocollimator and for the encoder outputs. The closed-loop bandwidth is 1.3 Hz for the autocollimator, and 0.6 Hz for the encoder. The rms error in 32 km/h wind is 0.43 mdeg at autocollimator, and 0.40 mdeg at the encoder.

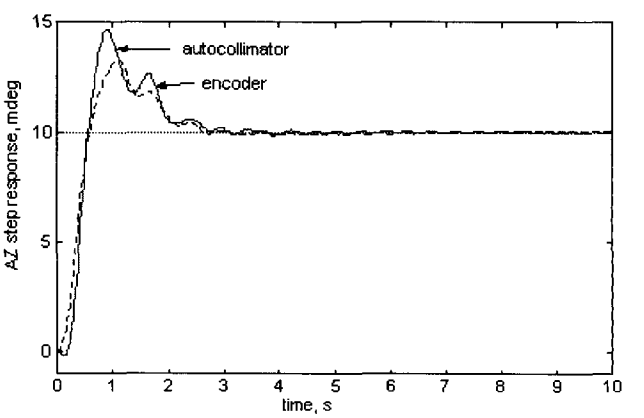

Figure 9. AE closed-loop responses of the autocollimator and the encoder to azimuth 10 mdeg step offset.

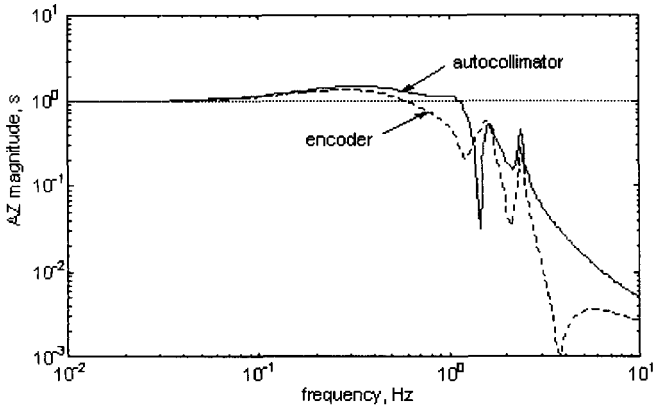

Figure 10. Magnitudes of the closed-loop transfer function, autocollimator and encoder, azimuth axis.

Elevation axis controller performance. The settling time for the 10-mdeg step of the elevation encoder and the elevation autocollimator is 2.2 s in both cases, overshoot is 35% at autocollimator and 22% at encoder. The closed-loop bandwidth is 1.8 Hz for the autocollimator, and 0.8 Hz for the encoder. The rms error in 32 km/h wind is 1.30 mdeg at autocollimator, and 1.21 mdeg at the encoder.

3.2. Master Equatorial Closed-Loop System

The ME control system has the same arrangement as the antenna system in Fig.7, where the antenna open-loop system is replaced with the ME open-loop system, and antenna controller is replaced with a proportional-and-integral controller with a feedforward loop. Its proportional gain is $k_p = 20$ and the integral gain is $k_i = 10$. The ME step response is shown in Fig.11. It has small overshoot (2%), and small settling time (0.2 s). The ME bandwidth is 3.5 Hz. The performance of the ME exceeds the antenna performance, as required. Namely, the ME settling time is much smaller than the antenna settling time, and the ME bandwidth is much wider than the antenna bandwidth. The wind disturbance rejection property is not of concern, since the ME is shielded from wind gusts.

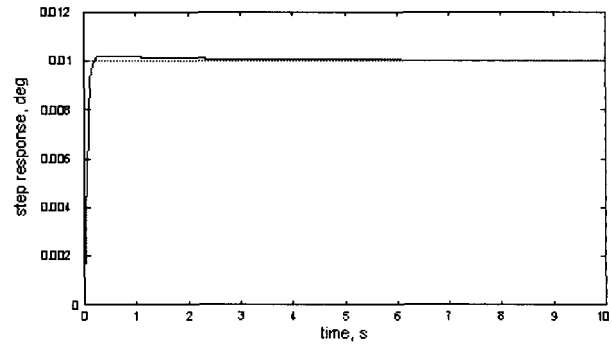

Figure 11. ME step response.

4. Modes of Interaction of the Antenna and Master Equatorial

There are three modes of operation of the antenna closed loop system. The simplest one, called Antenna Encoder (AE) mode, is shown in Fig.7; it is the stand-alone antenna closed-loop system where the ME is not involved. In this mode, antenna encoders are used to close the feedback loop. In order to improve the antenna tracking precision additional two modes are used. In these modes the ME is used as a part of the antenna tracking system, i.e., both antenna and ME interact during tracking. There are two types of interaction, or modes: the autocollimator (AC) mode, and ME encoder (MEE) mode. In the AC mode, as shown in Fig.3, the ME is commanded and antenna follows the ME using autocollimator as a position sensor. The antenna can be switched from AC to AE mode, as shown in Fig.3. In the MEE mode, shown in Fig.12, the antenna is commanded and the ME follows the antenna using the autocollimator as a coupling device. The ME encoder serves as a position sensor for the antenna. This mode can also be switched to the AE mode, as shown in Fig.12.

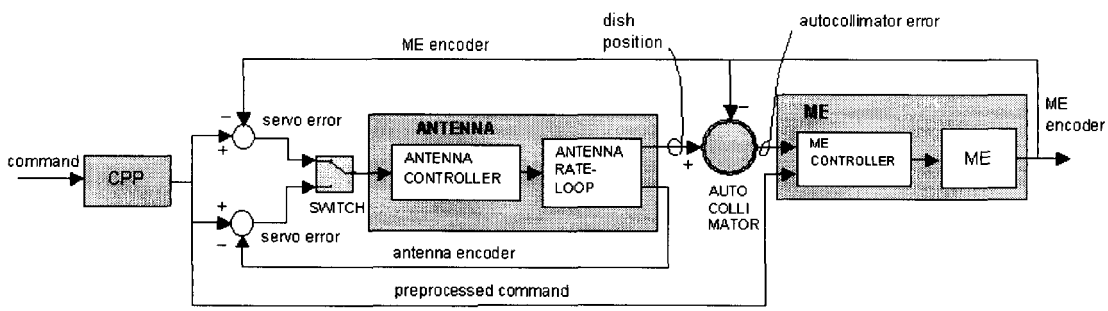

Figure 12. MEE mode (switch at the upper position), and AE mode (switch at the lower position)

The main disadvantage of the AC mode is the ability to decouple of the ME and the antenna if the autocollimator acquisition is lost. It can happen because the ME, as a small and rigid device, is much faster (up to 2 deg/s) than the heavy and flexible antenna (up to 0.25 deg/s). Therefore, in certain situations (such as tracking near keyhole) the autocollimator signal is outside the acquisition range, disabling the autocollimator as a sensor. In this situation the autocollimator mode is switched into the encoder mode. The switching itself, as well as encoder usage, reduces the tracking precision.

In the MEE mode the ME follows the antenna. Since the ME is much faster than the antenna, it will virtually never be left behind, and the autocollimator coupling will not be disconnected. In this mode (shown in Fig.12) the ME serves as the antenna position sensor (replacing the antenna encoders).

In the following section we present the results of the simulated performance of the AC and MEE modes. We tested the autocollimator errors using small steps (0.01 deg) and large rate offsets (0.2 deg/s=80% of max rate). Small commands verify the antenna linear dynamics, and assure that the system behaves similarly to the antenna closed-loop system without the ME. Large commands verify the magnitudes of the autocollimator errors (shall be smaller than allowed 110 mdeg).

The autocollimator errors for 10-mdeg steps are shown in Fig.13, solid line for the AC mode, and dashed line for the MEE mode. They are similar to the antenna response in the AE mode (without ME), except there are no vibrations visible in Fig.13 due to the smoothing action of the command preprocessor.

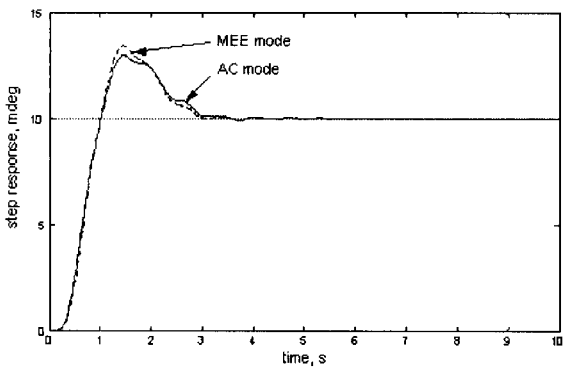

Figure 13. Autocollimator responses to 10 mdeg steps for AC mode (solid line) and MEE mode (dashed line).

The autocollimator errors for 0.2 deg/s are shown in Fig.14, solid line for the AC mode, and dashed line for the MEE mode. For the AC mode the error is large (its max value is 63 mdeg) and for the MEE mode the error is small (its max value is 2.5 mdeg). The small error in the MEE mode can be explained by the fact that in MEE mode the ME follows the antenna and ME low inertia allows for fast following. In AC mode the antenna follows the ME, and antenna large inertia results in slow following and large autocollimator errors. One can see that for the fast movements of the antenna the MEE mode is more appropriate.

Additionally, for both modes we simulated the servo error measured at the autocollimator due to 32 km/h wind gusts. In AC mode the rms error is 0.37 mdeg (in azimuth) and 1.47 mdeg (in elevation, and in MEE mode it is 0.38 mdeg (in azimuth) and 1.52 mdeg (in elevation).

5. Switching Modes Near the Keyhole

The axes of rotation of antenna and ME are not identically oriented: the antenna rotates with respect to azimuth and elevation axes while the ME rotates with respect to hour and declination axes. In order to allow mutual cooperation we implemented a coordinate translator. Additional difficulties appear due to existence of different keyholes, or singular points, for each coordinate system. Tracking through (or near) the keyholes requires high rates that exceed the imposed rate limits. Thus, antenna rates near the antenna keyhole, or ME rates near the ME keyhole are too low, thus the servo errors grow to unacceptable values. The 70-m antennas keyhole is at elevation position of 90 deg, and the ME keyhole is at declination position of 90 deg (which corresponds to azimuth position of 0 deg and elevation position of 35.425 deg at Goldstone – the California site of NASA antennas). For more about tracking close to the keyholes see Ref.[9].

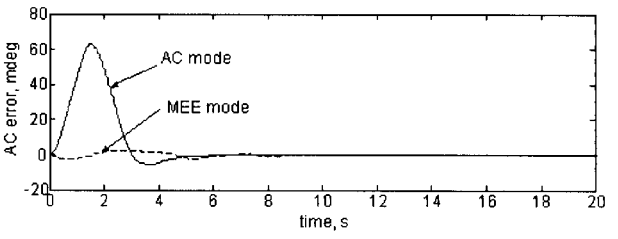

Figure 14. Autocollimator errors due to 0.2 deg/s rate offset for AC and MEE modes.

Near the keyhole the ME is not fast enough, causing antenna lagging (in AC mode), or antenna instability (in MEE mode). In order to prevent lagging or instability, it is recommended to switch near the keyhole from MEE or AC into AE mode. Since the hour servo error of ME grows significantly near the ME keyhole, the moment of switching is determined by measuring this error: the switch is triggered when the hour error exceeds the specified threshold of 0.2 deg. In the following sections we analyze the antenna dynamics during and after switching, from AC to AE mode and from MEE to AE mode.

5.1. Switching from AC to AE mode

In AC mode we add a filter to smooth jitter after switching. In this mode the ME is outside the antenna feedback loop, therefore filter addition does not destabilize the antenna.

The control system consists of:

- command preprocessors in azimuth and elevation (CPP AZ and CPP EL),
- ME control system in hour-declination coordinates. Although its inputs and outputs are in azimuth-elevation coordinates the internal dynamics is in the hour-declination coordinates; the hour error is an additional ME output that triggers the switches.
- azimuth and elevation switches,
- filters (Filter AZ and Filter EL), that process jerky azimuth and elevation positions after switching,
- antenna control systems in azimuth and elevation (marked Antenna AZ and Antenna EL)

This control system is similar to the one shown in Fig.3, except for the filter right after the switch. A filter of bandwidth is 0.28 Hz smoothes the jerks see Ref. [2]. Its transfer function is as follows

$$G(s) = \frac{15}{s^3 + 6s^2 + 15s + 15}$$

Normally the switch is at the upper position. In this position the ME is part of the system, and the ME position is compared with the antenna position (using the autocollimator). The resulting servo error (at autocollimator) closes the feedback loop. When the ME hour error exceeds the threshold value of 0.2 deg the switch is moved to the lower position. With the switch at the lower position the ME is bypassed, and the command is directly transmitted into the antenna and compared with the antenna encoder position to close the feedback loop. However, the ME continues to track, thus when the autocollimator error is small enough, the control is switched back to the AC mode. In this way, the switch at the upper position engages autocollimator and at the lower position engages the antenna encoders, to close the feedback loop.

In order to simulate and observe the switching near the keyhole we keep the antenna at the constant azimuth position of 0.6 deg, and move it upward in elevation at rate of 0.1 deg/s, starting from the elevation position of 34 deg. In this movement the ME is positioned close to the keyhole, and the hour error exceeds the threshold value of 0.2 deg. Indeed, the plot of the hour error in Fig.15 shows two time segments of the crossing the value of ±0.2 deg. One appears at time between 21 and 25 s (three crossings observed at 21.2 s, 21.8 s, 24.8 s) and the second at the time between 99 s and 102.2 s (five crossings observed at 99.0 s, 99.3 s, 100.9 s, 101.4 s, 102.2 s). As we see, typically multiple switches occur when transferring from autocollimator to antenna encoder mode.

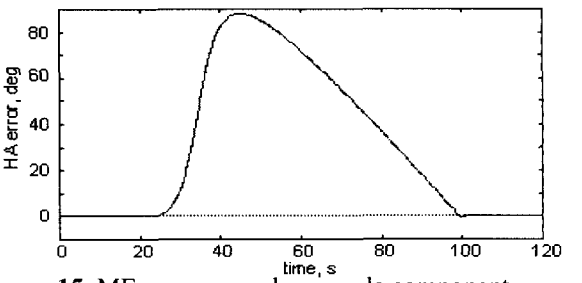

Figure 15. ME servo error, hour angle component.

The plot of the azimuth signal just after the Switch AZ is shown in Fig.16, with multiple switching in form of spikes. The filter smoothes the spikes, see the azimuth signal after the filter in Fig.17. Similar results were obtained for the elevation axis.

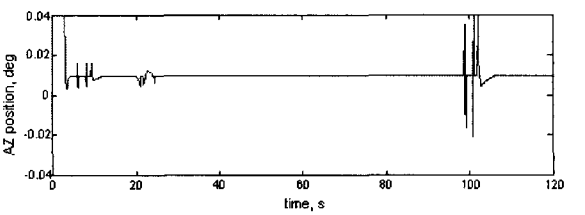

Figure 16. Switching modes: antenna azimuth position before filter.

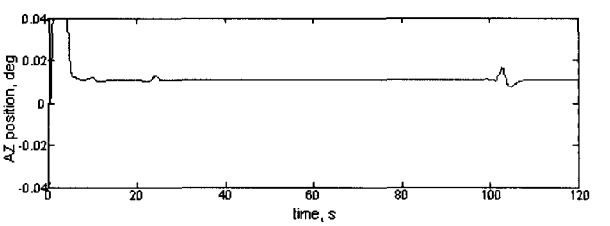

Figure 17. Switching modes: antenna azimuth position after filter, AC mode.

5.2. Switching from MEE to AE mode

In MEE mode the ME is a part of the antenna feedback loop, and its modification impacts the antenna performance and even stability. Thus, adding an additional filter after the switch will cause deterioration of the tracking precision or instability of the system. For this reason the MEE mode is left without filters that smoothed the switching jerks in AC mode.

The performance of the MEE mode when switching near the ME keyhole is analyzed similarly to the AC mode. The switch is triggered at time 25.5 s and 101-105 s. Fig.18 show the antenna azimuth position. The error during the first switch is less than 2 mdeg and no multiple switching appeared; the error at the second switch (at time 101s) is larger – up to 25 mdeg but

reduced two-fold due to the antenna closed-loop properties.

Comparing the AC and MEE modes we see that the switching errors are of comparable amplitudes – despite the lack of filter in MEE mode. This phenomenon is due to the disturbance rejection properties of the closed-loop system: in MEE mode the switching jerks are within the loop. In AC mode they were outside the loop, and they were suppressed by the added filter.

6. Conclusions

In this paper we described and analyzed three modes of the 70-meter antenna control system. The goal was to obtain a single control algorithm to track and to slew in all three modes. The goal was achieved by taking the following steps.

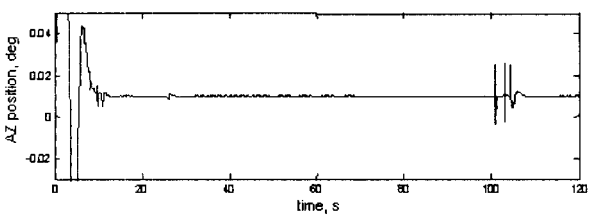

Figure 18. Switching modes: antenna azimuth position, MEE mode

First, we developed accurate antenna and ME models using the test results and system identification procedure. In consequence we developed the LQG controllers that significantly improved the tracking precision of the antenna.

Next, we analyzed two modes of interaction of the antenna and ME: AC mode (where slave antenna follows master ME) and MEE mode (where slave ME follows master antenna). The analysis shows that both modes work satisfactorily using a single control algorithm. Namely, AC mode with the addition of the command preprocessor can be used in slewing, tracking, and scanning since the maximal autocollimator error is less than 110 mdeg (peak-to-peak), thus smaller than the max allowable error of 220 mdeg. However, for MEE mode the analysis shows that autocollimator errors are very small (less than 2 mdeg peak-to-peak), and that this mode is better fitted for slewing, tracking and scanning.

Finally, we simulated the switching between the AC and AE modes and between MEE and AE modes. The analysis showed that switching jerks are small, both in AC mode and MEE modes.

Comparison of AE, AC and MEE modes. The location of the antenna encoders prevents the accurate measurement of the RF beam position, due to significant flexible deformation of the antenna structure between the encoder locations and the RF beam location (antenna focal point). For this reason the AE mode is used only as a backup mode. The AC mode is currently used and the main concern is its deactivation when the servo error exceeds 110-mdeg threshold. This happens near the ME keyhole. We showed that the MEE mode has much smaller servo error therefore it has less tendency to disengage.

Acknowledgements

We would like to thank David Girdner and Robert Haroldsson (Honeywell) for technical discussions and assisting in the antenna testing and measurements, and Martha Berg and Stephen Slobin (JPL) for their discussions in the azimuth/elevation to hour/declination transformation analysis. The research described in this paper was carried out at the Jet Propulsion Laboratory, California Institute of Technology, under a contract with the National Aeronautics and Space Administration.

References

[1] Gawronski, W., "Control and Pointing Challenges of the Deep Space Network Antennas," *8th IEEE Int. Conf. On Methods and Models in Automation and Robotics,* Szczecin, Poland, Sept. 2002.

[2] Juang, J.N., Horta, L.G., and Phan M., "System/Observer/Controller Identification Toolbox," NASA Tech Memo 107566, 1992.

[3] Juang, J.N., *Applied System Identification,* Prentice Hall, Englewood Cliffs, 1994.

[4] Gawronski W., "Antenna Control Systems: from PI to H_∞," *IEEE Antennas and Propagation Magazine*, Vol.43, No.1, 2001.

[5] Gawronski W., "Linear Quadratic Controller Design for the Deep Space Network Antennas," *Journal of Guidance, Control, and Dynamics*, Vol.17, No.4, 1994.

[6] Gawronski, W., Ahlstrom Jr., H. G., and Bernardo, A., "Design and Performance of the DSS-14 Antenna Controller," NASA TMO Progress Report, Vol.42-135, 1998, http://tmo.jpl.nasa.gov/tmo/progress_report/42-135/135E.pdf.

[7] Gawronski, W., and Almassy, W. "Command Pre-Processor for Radiotelescopes and Microwave Antennas," *IEEE Antennas and Propagation Magazine*, Vol.44, No.2, 2002.

[8] Nickerson, J.A., "New Mode Switching Algorithm for the JPL 70-Meter Antenna Servo Controller," NASA TDA Progress Report, Vol. 42-92, 1987. http://tmo.jpl.nasa.gov/tmo/progress_report/42-92/92Q.PDF

[9] Gawronski, W., "70-Meter Antenna Tracking and Mode Switching Near the Master Equatorial Keyhole" NASA IPN Progress Report, Vol. 42-148, 2002, http://ipnpr.jpl.nasa.gov/tmo/progress_report/42-148/148C.pdf